

## New Calibration of the Ruby Pressure Scale based Primarily on Shock-Wave-Reduced Isotherms

*Akobuije D. Chijioke<sup>1</sup>, W.J. Nellis<sup>1</sup>, A. Soldatov<sup>1,2</sup>, and Isaac F. Silvera<sup>\*1</sup>,*  
<sup>1</sup>Harvard University, Lyman Laboratory of Physics, Cambridge, MA, USA,

<sup>2</sup>Department of Applied Physics and Mechanical Engineering, Lulea University of  
 Technology, SE 971 87 Sweden [silvera@physics.harvard.edu](mailto:silvera@physics.harvard.edu)

We present our recent new calibration of the ruby pressure scale based on experimentally obtained reference curves. We discuss important points for accurate calibration of the ruby gauge: use of an appropriate experimentally-based calibration method, use of quasi-hydrostatic data, and the question of the fitting form used for extrapolation.

### I. INTRODUCTION

The shift of the ruby fluorescence R-line with pressure, proposed as a practical pressure gauge by Forman et al. (1972), has enabled widespread quantitative ultra-high pressure experiments using diamond anvil cells. The accuracy of the experimental results obtained using this scale depends upon the accuracy of the calibration of the ruby gauge.

We have recently presented a revised calibration of the ruby fluorescence pressure gauge under quasi-hydrostatic compression (Chijioke et al., 2005b). This calibration was based on using experimental pressure references. Data used for the calibration were published data for ruby lineshift versus absolute pressure by Zha et al. (2000) published data for ruby lineshift versus volume of metal markers by Dewaele et al (2004), and our own measurements of

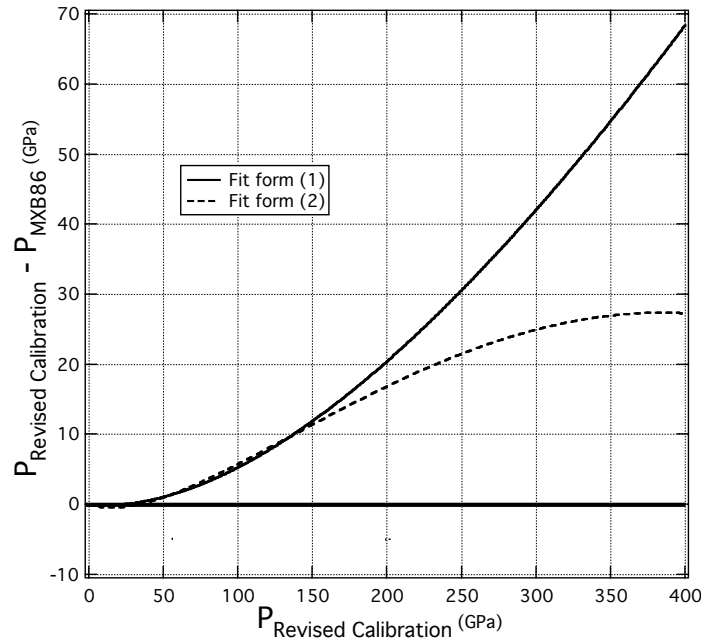


Figure 1. Difference between revised ruby scale and the currently used scale of (Mao et al., 1986). The difference is shown for the two fit forms (1) and (2), which differ in the pressure indicated above the 150 GPa limit of the calibration.

ruby lineshift versus volume of a gold marker. The metal volume data were converted to pressure using equations of state (EOSs) determined from shock wave and ultrasonic data in our recent study (Chijioke et al., 2005a) and from shock wave data in the recent work of Wang et al (2002). A fit of the pressure as a function of ruby lineshift up to 150 GPa to the form

$$P = \frac{A}{B} \left[ \left( \frac{\lambda}{\lambda_0} \right)^B - 1 \right] \quad (1)$$

yields coefficients  $A = 1873 \pm 6.7$  GPa and  $B = 10.82 \pm 0.14$ . A fit to a second order polynomial

$$P = A \left[ \left( \frac{\Delta\lambda}{\lambda} \right) + B \left( \frac{\Delta\lambda}{\lambda} \right)^2 \right] \quad (2)$$

yields coefficients  $A = 1794 \pm 8.4$  GPa and  $B = 8.68 \pm 0.15$ . In Figure 1 we show the difference between the revised calibration and the previously widely-used calibration (Mao et al., 1986) with  $A = 1904$  and  $B = 7.665$  in form (1).

In the remainder of this paper we consider in more detail the question of accurate calibration of the ruby pressure gauge. In section II we critically discuss various methods of calibration and in section III we present the various calibration data in the literature and indicate the basis of our selection of data sets used in the calibration. In section IV we present and briefly discuss the shock-wave-reduced isotherms (SWRIs) that we have used for the calibration. In section V we consider calibration of the ruby gauge based on the extrapolated equation of state of diamond, which a number of authors have done. In section VI we consider the form of the equation fit to the ruby calibration data, which is relevant to extrapolation of the scale beyond the region of calibration.

## II. CALIBRATION METHODS

To calibrate the ruby gauge, the wavelength of fluorescent emission must be measured in an experiment simultaneously with a measurement of applied pressure. There are different methods for determining pressure, with the most fundamental methods being the most valid for calibration. In order of validity, acceptable ways of determining pressure for a calibration are (i) absolute pressure measurement via the free-piston gauge, (ii) absolute pressure calibration based on a thermodynamic relation among measured properties, and (iii) equations of state obtained from fundamental measurements at conditions close to those being considered, such as shock-wave-reduced isotherms. Additional methods sometimes used to determine pressure are (iv) equations of state extrapolated far from the conditions of measurement and (v) theoretical equations of state. These last two methods are not deemed appropriate for calibration given the availability of the more fundamental pressure measurements. It is also possible to transfer to ruby the calibration from another secondary gauge, such as another material with pressure-dependent fluorescence; in this case the validity of the ruby calibration depends upon the calibration of the initial secondary gauge.

### A. Free piston gauge

If a hydrostatic medium is compressed in a piston-cylinder chamber, the pressure is given absolutely by

$$P = \frac{F}{A} \quad (3)$$

where  $F$  is the force applied to the medium by the piston and  $A$  is the cross-sectional area of the piston, both related to fundamental standards. However this technique is restricted to low pressures because at pressures greater than a few GPa, friction and deformation in piston-cylinder devices lead to large corrections and uncertainties.

### B. Thermodynamic relation

As described by Decker and Barnett in 1970 (Decker and Barnett, 1970) and Ruoff et al in 1973 (Ruoff et al., 1973), an empirical pressure parameter can be calibrated against absolute pressure using a thermodynamic relation among thermodynamic properties which vary with pressure, if these properties can all be measured as a function of the empirical pressure parameter. In particular, the definition of the bulk modulus

$$B_T = -V \left( \frac{\partial P}{\partial V} \right)_T = B_S / \left( 1 + \frac{\alpha^2 V B_S T}{C_P} \right) \quad (5)$$

has been used, where  $B_T$  is the isothermal bulk modulus,  $B_S$  is the adiabatic bulk modulus,  $\alpha$  is the volume coefficient of thermal expansion,  $V$  is the volume,  $T$  is the temperature and  $C_P$  is the constant-pressure specific heat. Zha et al (2000) have used this technique on MgO to calibrate ruby under pressure to 55 GPa.

### C. Shock-wave-reduced isotherms

X-ray measurement of the volume of a marker material with a known EOS, which is compressed, together with a piece a ruby in the experimental cell, provide a means of determining pressure. Mao et al (1978) introduced the technique of using SWRIs as EOSs to calibrate the ruby pressure gauge. Shock wave experiments measure stress-volume-energy data points in the EOS space of a material via the Rankine-Hugoniot relations (see for example McQueen et. al. (1970)). In the region up to 300 GPa for metals and other relatively incompressible substances, these data points are not far removed from the isotherm of the material. A relatively small temperature correction and an even smaller stress correction convert the shock wave data to a room temperature  $P(V)$  isotherm.

### D. Extrapolated equations of state

Measurements of the elastic properties of a material at low pressures, such as are done by ultrasonic techniques, yield the bulk modulus of the material and its pressure derivative(s). The  $P(V)$  isotherm of the material can be extrapolated from these data to pressures above those at which the measurements were made. While the error in the isotherm thus obtained will be small at pressures not far above the range of the measurements, at higher pressures the error can become large; the accuracy of the equation of state then depends strongly on the extrapolation of the low-pressure data. Equations of state thus determined no longer satisfy the fundamental requirement for an experiment based calibration standard.

### E. Theoretical equations of state

It is also possible to derive the equation of state of a marker material completely theoretically, from first principles. The unsuitability of such equations of state for calibration is evident.

### III. RUBY CALIBRATION DATA

The ruby pressure gauge was first calibrated by Piermarini et al (1975) up to 20 GPa using the theoretical Decker equation of state of sodium chloride (Decker, 1971). Since then there have been several calibration lineshift-vs-pressure data sets generated and corresponding recalibrations of the ruby scale. These data sets are summarized in Table 1 and the ruby scales obtained from them are plotted in Figure 2.

The best data to use for calibrating the ruby scale are those obtained under the most nearly hydrostatic conditions. Non-hydrostaticity leads to pressure gradients in the sample, meaning that a ruby chip embedded at some location is not at the same pressure as all of the surrounding medium. Non-hydrostatic stress also alters the shift of the R-line wavelength with pressure, this shift being known to be different for uniaxial stresses in different crystallographic directions (He and Clarke, 1995, Chai and Brown, 1996). Under high pressures in the gigapascal range, all known materials are solid at room temperature, and thus do not provide a strictly hydrostatic environment for pressurization. However, some solids have sufficiently low yield strengths even at very high pressures to allow a distribution of stresses to be achieved that is close to hydrostatic. Helium is the best known such medium, followed by hydrogen. Neon is probably a reasonably good quasi-hydrostatic medium, but has not been studied for this property to high enough pressures.

Reference	Method	Pressure Limit
(Piermarini et al., 1975)	Marker (NaCl): theoretical EOS Methanol-ethanol medium	20 GPa
(Mao et al., 1978)	Marker (Ag, Cu, Mo, Pd): SWRI Methanol-ethanol medium	100 GPa
(Bell et al., 1986)	Marker (Cu, Au): SWRI and mixed EOS No medium	180 GPa
(Mao et al., 1986)	Marker (Ag, Cu): SWRI Argon medium	80 GPa
(Aleksandrov et al., 1987)	Marker (Diamond): extrapolated EOS Helium medium	40 GPa
(Hemley et al., 1989)	Marker (W): SWRI Neon medium	110 GPa
<b>(Zha et al., 2000)</b>	<b>Thermodynamic calibration using MgO Helium medium</b>	<b>55 GPa</b>
(Holzapfel, 2003)	Marker (Diamond, W): extrapolated EOS and SWRI, Helium and neon media	140 GPa
(Dorogokupets and Oganov, 2003)	Marker (Ag, Cu): SWRI Argon medium	80 GPa
<b>(Dewaele et al., 2004)</b>	<b>Marker (Al, Au, Cu, Pt, Ta, W): SWRI Helium medium</b>	<b>150 GPa</b>
<b>(Chijioke et al., 2005b)</b>	<b>Marker (Au): SWRI Xenon and hydrogen media</b>	<b>100 GPa</b>

Table 1. Ruby calibrations. Data sets used for the revised calibration are indicated in boldface.

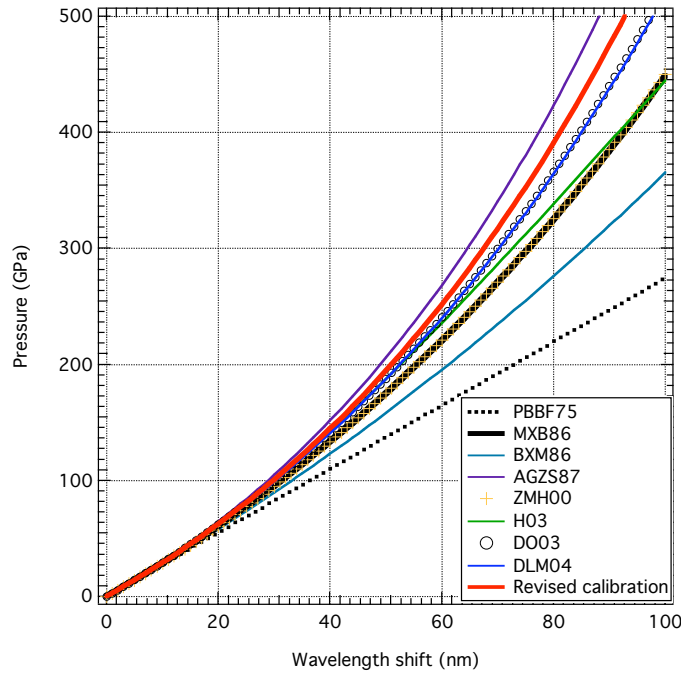


Figure 2. Calibrations of the ruby scale in references listed in Table 1, and our revised calibration as fit to form (1).

Xenon is also surprisingly a fairly good quasi-hydrostatic medium up to 100 GPa, probably due to an extended phase transition in the range up to 100 GPa (Cynn et al., 2001, Asuami and Ruoff, 1986) that allows redistribution of stresses. An alternative means of achieving quasi-hydrostatic pressurization is to melt the pressure medium after pressurization and then allow it to re-solidify and cool to room temperature before making pressure and ruby lineshift measurements.

From the data sets listed in Table 1, we select three as being most suitable for calibration. These are indicated in bold and are data sets obtained in quasi-hydrostatic media and in which pressure was determined either by thermodynamic relation or from volume measurements on pressure markers for which SWRIs are available. The data set of Dewaele et al (2004) is much more extensive than the others selected and therefore dominates the calibration. (Dewaele et al present 233 data points in a range up to 150 GPa, versus 28 data points up to 55 GPa by Zha et al (2000) and 9 data points up to 100 GPa from our study (Chijioke et al., 2005b)). As Dewaele et al. used pressure markers for which SWRIs are available as the means of determining pressure, the accuracy of the SWRIs is of critical importance to this calibration.

#### IV. SHOCK-WAVE-REDUCED ISOTHERMS

In shock-wave experiments, the quantities usually measured are the shock velocity  $u_s$  and velocity of the material after transit of the shock wave, known as the particle velocity  $u_p$ . These are related to the axial stress  $\sigma$ , Volume  $V$  and Energy  $E$  of the shocked material via the Rankine-Hugoniot equations:

$$\begin{aligned}\sigma - \sigma_0 &= \frac{1}{V_0}(u_s - u_0)(u_p - u_0) \\ V &= V_0 \left[ 1 - (u_p - u_0)/(u_s - u_0) \right] \\ E - E_0 &= \frac{1}{2}(P + P_0)(V_0 - V)\end{aligned}\quad (6)$$

where  $\sigma_0$ ,  $V_0$ ,  $E_0$  and  $u_0$  are the axial stress, volume, energy and velocity of the unshocked material. The locus of P-V-E points generated by shocks of varying strength from a single initial state of a material is called a Hugoniot. Reverberating-shock and ramped-pressure-profile (Barker, 1983) techniques allow shock compression to off-Hugoniot points such as points along an isentrope. Corrections for the effects of material strength and temperature “reduce” the shock-generated data points to a P-V isotherm.

In obtaining an isotherm from shock-wave data there are three items to be addressed: the accuracy of the shock data, the correction for the material strength, and the thermal correction. We address these three questions in turn for the materials of concern for the present calibration - aluminum, copper, gold, platinum, tantalum and tungsten.

#### (i) Hugoniot Data

The pressure region of concern for the present calibration is that up to 150 GPa. Within this region, the most accurate Hugoniot data available in the literature are shown in Table 2. The Hugoniot data are presented in the form of a linear fit to the data points

$$u_s = C + S \cdot u_p \quad (7)$$

Mitchell and Nellis (1981) reported data for Al, Cu and Ta with error bars and error analyses, and the 1-standard-deviation value of these at 150 GPa are shown in Table 2.

Metal	C (cm/s)	S	$\rho_0$ (g/cm <sup>3</sup> )	Range of validity (GPa on Hugoniot)	$\delta\sigma/\sigma$ (150 GPa)	Reference
Al	0.5386	1.339	2.707	8 - 200	0.020	(Mitchell and Nellis, 1981)
Cu	0.3933	1.500	8.939	16 - 330	0.009	(Mitchell and Nellis, 1981)
Ta	0.3430	1.19	16.66	26 - 222		(McQueen et al., 1970)
	0.3293	1.307	16.68	55 - 430	0.010	(Mitchell and Nellis, 1981)
W	0.4022	1.260	19.25	27 - 680		(Hixson and Fritz, 1992)
Au	0.307	1.54	19.24	25 - 190		(Marsh, 1980)
Pt	0.3641	1.541	21.41	32 - 660		(Holmes et al., 1989)

Table 2. Hugoniot data for SWRIs.

#### (ii) Strength correction

The shock data presented here were obtained under conditions of uniaxial compression, where the quantity given by the Rankine-Hugoniot equations is the stress in the direction of shock propagation. Because the materials being compressed are solids and thus have some strength, there is a small difference between this component of stress and the mean normal stress in the material, i.e. the pressure. This strength offset has been measured for Al (Asay et

al., 1986), and Cu, Ta and W (Chhabildas and Asay, 1992). The magnitude of this strength correction as a percentage of the pressure on the isotherm is plotted in Figure 3.

### (iii) Thermal correction

To reduce a Hugoniot to an accurate isotherm, the relative magnitude of the thermal pressure generated by shock compression should be as small as possible. This thermal pressure increases with the compressibility of the material under study and with pressure along the Hugoniot. Over the years there have been numerous calculations of the thermal pressure, of varying sophistication. Wang et al (2002, 2004) have done recent first-principles calculations of this pressure for the materials under consideration using a classical mean field potential model in which all thermal contributions are included self-consistently. These thermal pressures are plotted as percentages of pressure on the isotherm in Figure 4. The maximum thermal pressure in the range under consideration is 32% for aluminum at 150 GPa. For the other materials under consideration it is less than 25% up to 150 GPa.

The isotherms thus generated for Al, Cu, Ta and W have been fit to the form

$$P = 3K_0 \left[ \frac{1 - X^{1/3}}{X^{2/3}} \right] \exp \left[ \eta(1 - X^{1/3}) + \beta(1 - X^{1/3})^2 + \xi(1 - X^{1/3})^3 + \delta(1 - X^{1/3})^4 \right]$$

where  $X = V/V_0$ , with coefficients tabulated in Table 3. As shown in Table 2, the Hugoniot data used is valid from some elevated pressure (ranging from 8 GPa for aluminum to 27 GPa for Tungsten) up to an upper pressure limit. To obtain isotherms that are accurate down to ambient pressure we fixed the bulk modulus in the fits shown in Table 3 to the ultrasonically measured values (Katahara et al., 1979, van't-Klooster et al., 1979, Tallon and Wolfenden, 1979). Thus the fits

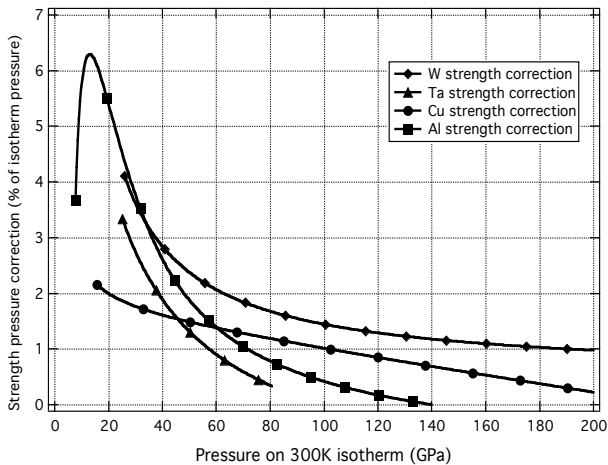


Figure 3. Hugoniot strength corrections as a percentage of pressure on the isotherm.

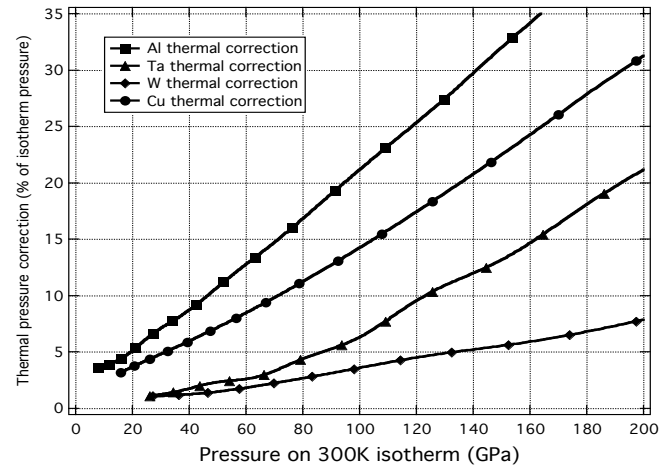


Figure 4. Thermal corrections to reduce Hugoniot to isotherm, as a function of pressure on the isotherm.

represent combined shock- and ultrasonically-derived isotherms, the data from each type of experiment are used only in the region of validity. Also shown in Table 3 are fits to isotherms for Au and Pt generated by Wang et al (2002) which incorporate thermal correction but no strength correction, and which we have used in the present ruby calibration. In Figure 5 we show the deviation between the fits given in Table 3, used for the ruby calibration, and the actual reduced shock data. This deviation is seen to be generally less than 0.5 GPa throughout the range of the SWRI.

As noted above, with increasing pressure on the Hugoniot the relative magnitude of the thermal pressure increases, and ultimately diverges (Rozsnyai et al., 2001). Thus the thermal pressure limits the fundamental accuracy of isotherms obtained from Hugoniots for pressures much higher than those considered here. Isentropic shock compression [e.g.(Asay et al., 1986)], however, enables high compression to be achieved with greatly reduced thermal pressure, at the cost of a somewhat increased material strength correction. Isentropic compression thus provides a means for obtaining calibration-quality shock-derived-isotherms to much higher pressures.

Material	$K_0$	$\eta$	$\beta$	$\xi$	$\delta$	Pressure limit	Reference
Al	72.6	4.1267	26.1269	-154.33	326.69	200 GPa	(Chijioke et al., 2005a)
Cu	133.3	5.4167	15.921	-90.223	235.81	200	(Chijioke et al., 2005a)
Ta	194.1	1.9265	52.348	-402.72	1031.5	300	(Chijioke et al., 2005a)
W	308.6	2.7914	45.694	-409.97	1290.2	300	(Chijioke et al., 2005a)
Au	177.26	6.3800	1.9334	-1.0292	33.941	513	(Wang et al., 2002)
Pt	280.03	6.3289	-1.3811	61.492	-156.48	660	(Wang et al., 2002)

Table 3. Isotherms used for ruby scale calibration.

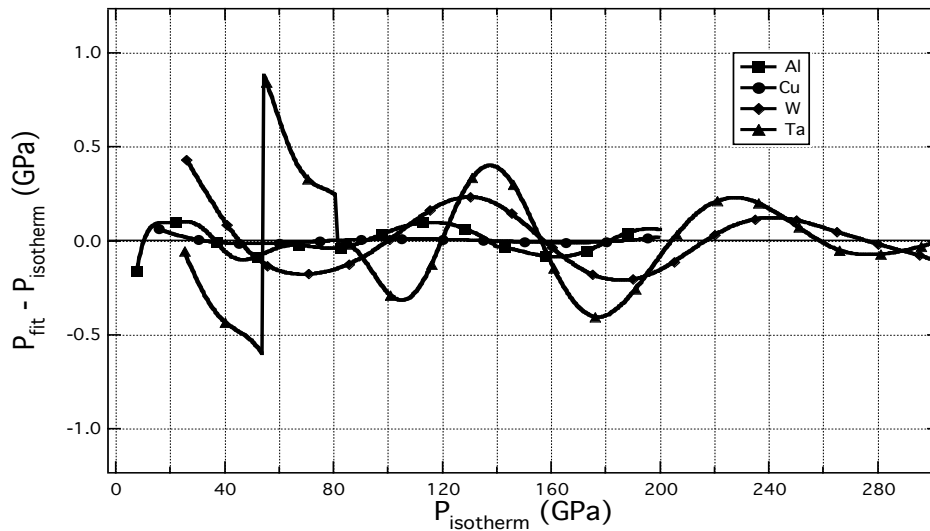


Figure 5. Residual difference between the shock wave reduced isotherms obtained and the fits given in Table 3. The discontinuity in the residual for Ta results from the use of one Hugoniot curve below 55 GPa and another above 55 GPa, with a slight mismatch between the two Hugoniots at 55 GPa.

## V. CALIBRATION USING THE EXTRAPOLATED EQUATION OF STATE OF DIAMOND

Recalibrations of the ruby scale have been proposed based on the equation of state of diamond (Aleksandrov et al., 1987, Holzapfel, 2003). The equation of state used is based on ultrasonic measurements of  $K_0$  and  $K_0'$ , the bulk modulus and its derivative at zero pressure, extrapolated up to high pressure. Generally, an equation of state extrapolated to conditions far beyond the range of measurement is not appropriate for calibration, as the EOS is largely based on the extrapolation. However the highly incompressible nature of diamond is favorable in this regard, as the compressions are still small at high pressures (~15% volumetric compression at 100 GPa) and therefore the extrapolation may retain some validity within this pressure range. As a result, within this range the EOS is relatively insensitive to the extrapolation form. Thus, although extrapolation is not supported on principle as a means of calibration, as a practical matter an extrapolated equation of state of diamond based on ultrasonic measurements could be a fairly accurate reference up to ~100 GPa.

However such extrapolated equations of state depend sensitively on the accuracy of the ultrasonic measurements. While there is high confidence in the ultrasonic value of the bulk modulus  $K_0$ , the present uncertainty in its derivative  $K_0'$  is estimated at ~12.5% (McSkimin and Andreatch, 1972), leading to an intolerably large uncertainty at pressures above ~ 60 GPa.

## VI. FITTING FORM OF THE RUBY SCALE FOR EXTRAPOLATION

Within the range of the calibration, any form with sufficient flexibility to fit the data is acceptable. However current diamond cell experiments often go to pressures above 200 GPa and occasionally to pressures above 300 GPa, whereas the ruby scale is calibrated only to 150 GPa. Thus, it is necessary to extrapolate beyond the range of the calibration, making important the details of the fitting form used. Techniques developed by Chen and Silvera (1996) and Eggert et al (1991, 1988) enable the measurement of ruby fluorescence to pressures above 250 GPa.

Up to the present 150 GPa limit of calibration, we have found that two parameters are sufficient to fit the calibration data. The simplest such form is a second order polynomial, Eq. (2). Other forms may result from various assumptions or theoretical models. In particular, the form Eq. (1) introduced by Mao et al (1978) and used in most subsequent calibrations results from the assumption that  $\partial P/\partial(\ln\lambda)$  is a linear function of pressure. This added constraint leads to higher extrapolated pressures than with a polynomial.

Holzapfel (2003) proposed the three-parameter form

$$P = \frac{A}{B+C} \left( \exp \left\{ \frac{B+C}{C} \left[ 1 - \left( \frac{\lambda}{\lambda_0} \right)^{-C} \right] \right\} - 1 \right) \quad (9)$$

which reduces to the form (1) in the limit  $C \rightarrow 0$ . The primary effect of the additional parameter is to increase the flexibility of the fit, allowing a change in curvature at high pressures.

In general, any form to be used in preference to the polynomial Eq. (2) should have some theoretical justification. Such theoretically-motivated forms might in principle be obtained by combining an appropriate form for the P-V EOS with an appropriate form for the level shift as a function of volume. So far there has not been established along these lines an accepted form for the pressure as a function of lineshift. In this regard it may be noted that a two-term Taylor expansion of the pressure as a function of volume about the zero pressure point

$$P(V) = K_0 \left[ \left( \frac{V_0 - V}{V} \right) + \frac{K_0' - 1}{2} \left( \frac{V_0 - V}{V} \right)^2 \right] \quad (10)$$

yields the quadratic  $P(\lambda)$  form Eq. (2) if the R-line energy level scales linearly with volume.

The P-V form (10) has been indicated by Syassen (2004) to be appropriate for pressures up to ~ 200 GPa or greater, while Eggert et al (1989) have found support for a linear variation of the R-line level with volume in the context of a crystal field analysis.

Further investigation may lead to a more strongly justified analytical form for the ruby lineshift as a function of pressure. For the present we propose to continue using the form Eq. 1 that does a good job in fitting the data up to 150 GPa and has been widely used by the community.

## VII. CONCLUSION

We have combined available quasi-hydrostatic ruby lineshift data with improved shock-wave-reduced isotherms to provide a new calibration of the ruby pressure scale. The revised scale indicates higher pressures at a given lineshift than the widely used calibration MXB86 (Mao et al., 1986), in broad agreement with the conclusions of several investigators. We have discussed the question of appropriate methods of determining pressure for a calibration and the question of the fitting form for the ruby scale.

## VII. ACKNOWLEDGEMENTS

We thank K. Syassen for useful comments and communication of unpublished notes. This work has received support from the Army Missile Command in the form of a TEAMS grant.

## REFERENCES

- ALEKSANDROV, I. V., GONCHAROV, A. F., ZISMAN, A. N. & STISHOV, S. M. (1987) Diamond at high pressures: Raman scattering of light, equation of state, and high-pressure scale. *Sov. Phys. JETP*, 66, 384-390.
- ASAY, J. R., CHHABILDAS, L. C., KERLEY, G. I. & TRUCANO, T. G. (1986) High Pressure Strength of Shocked Aluminum. IN GUPTA, Y. M. (Ed.) *Shock Waves in Condensed Matter*. New York, Plenum Press.
- ASUAMI, K. & RUOFF, A. L. (1986) Nature of the state of stress produced by xenon and some alkali iodides when used as pressure media. *Phys. Rev. B*, 33, 5633.
- BARKER, L. M. (1983) High pressure quasi isentropic impact experiments. *Shock Waves in Condensed Matter*. Elsevier, NY, 1984.
- BELL, P. M., XU, J. A. & MAO, H. K. (1986) Static Compression of Gold and Copper and Calibration of the Ruby Pressure Scale to Pressures to 1.8 Megabars. IN GUPTA, Y. M. (Ed.) *Shock Waves in Condensed Matter*. New York, Plenum.
- CHAI, M. & BROWN, J. M. (1996) Effects of static non-hydrostatic stress on the R lines of ruby single crystals. *Geophysical Research Letters*, 23, 3539-42.
- CHEN, N. H. & SILVERA, I. F. (1996) Excitation of Ruby Fluorescence at Multimegabar Pressures. *Rev. Sci. Instrum.*, 67, 4275-4278.
- CHHABILDAS, L. C. & ASAY, J. R. (1992) Dynamic Yield Strength and Spall Strength Measurements Under Quasi-Isentropic Loading. IN MEYERS, M. A., MURR, L. E. & STAUDHAMMER, K. P. (Eds.) *Shock-Wave and High-Strain-Rate Phenomena in Materials*. New York, Marcel Dekker.
- CHIJOKE, A., NELLIS, W. J. & SILVERA, I. F. (2005a) High Pressure Equations of State of Several Metals. *submitted for publication*.
- CHIJOKE, A., NELLIS, W. J., SOLDATOV, A. & SILVERA, I. F. (2005b) The Ruby Pressure Standard. *submitted for publication*.
- CYNN, H., YOO, C. S., BAER, B., IOTA-HERBEI, V., MCMAHAN, A. K., NICOL, M. & CARLSON, S. (2001) Martensitic fcc-to-hcp transformation observed in xenon at high pressure. *Phys. Rev. Lett.*, 86, 4552-4555.
- DECKER, D. L. (1971) *J. Appl. Phys.*, 42, 3239.
- DECKER, D. L. & BARNETT, J. D. (1970) Proposed thermodynamic pressure scale for an absolute high pressure calibration. *J. Appl. Phys.*, 41, 833.
- DEWAELE, A., LOUBEYRE, P. & MEZOUAR, M. (2004) Equations of state of six metals above 94 GPa. *Phys.Rev. B*, 70, 094112.
- DOROGOKUPETS, P. I. & OGANOV, A. R. (2003) Equations of State of Cu and Ag and revised ruby pressure scale. *Doklady Earth Sciences*, 391A, 854.
- EGGERT, J. H., GOETTEL, K. A. & SILVERA, I. F. (1988) Elimination of Pressure-Induced Fluorescence in Diamond Anvils. *Appl. Phys. Lett.*, 53, 2489.
- EGGERT, J. H., GOETTEL, K. A. & SILVERA, I. F. (1989) Ruby at High Pressure I: Optical Line Shifts to 156 GPa. *Phys. Rev. B*, 40, 5724.

- EGGERT, J. H., MOSHARY, F., EVANS, W. J., GOETTEL, K. A. & SILVERA, I. F. (1991) Ruby at High Pressure III. A New Pumping Scheme for the R Lines up to 230 GPa. *Phys. Rev. B*, 44, 7202.
- FORMAN, R. A., PIERMARINI, G. J., BARNETT, J. D. & BLOCK, S. (1972) Pressure Measurement Made by the Utilization of Ruby Sharp-Line Luminescence. *Science*, 176, 284-285.
- HE, J. & CLARKE, D. R. (1995) The piezo spectroscopic coefficients for Cr doped sapphire. *J. Am. Chem. Soc.*, 78, 1347.
- HEMLEY, R. J., ZHA, C. S., JEPHCOAT, A. P., MAO, H. K., FINGER, L. W. & COX, D. E. (1989) X-ray diffraction and equation of state of solid neon to 110 GPa. *Phys. Rev. B*, 39, 11820-11827.
- HIXSON, R. S. & FRITZ, J. N. (1992) Shock compression of Tungsten and Molybdenum. *J. Appl. Phys.*, 71, 1721.
- HOLMES, N. C., MORIARTY, J. A., GATHERS, G. R. & NELLIS, W. J. (1989) The EOS of Pt to 660 GPa (6.6 Mbar). *J. Appl. Phys.*, 66, 2962-2967.
- HOLZAPFEL, W. B. (2003) Refinement of the ruby luminescence pressure scale. *J. Appl. Phys.*, 93, 1813-1818.
- KATAHARA, K. W., MANGHNANI, M. H. & FISHER, E. S. (1979) Pressure derivatives of the elastic moduli of BCC Ti-V-Cr, Nb-Mo, and Ta-W alloys. *J. Phys. F.: Metals Physics*, 9, 773-790.
- MAO, H. K., BELL, P. M., SHANER, J. W. & STEINBERG, D. J. (1978) Specific Volume Measurements of Cu, Mo, Pd, and Ag and Calibration of the Ruby R<sub>1</sub> Fluorescence Pressure Gauge from 0.06 to 1 Mbar. *J. Appl. Phys.*, 49, 3276-3283.
- MAO, H. K., XU, J. & BELL, P. M. (1986) Calibration of the Ruby Pressure Gauge to 800 kbar Under Quasi-Hydrostatic Conditions. *J. Geophys. Res.*, 91, 4673-4676.
- MARSH, S. P. (Ed.) (1980) *Los Alamos Shock Hugoniot Data*, Berkeley, CA, University of California Press.
- MCQUEEN, R. G., MARSH, S. P., TAYLOR, J. W., FRITZ, J. N. & CARTER, W. J. (1970) High-Velocity Impact Phenomena. IN KINSLOW, R. (Ed.) New York, Academic.
- MCSKIMIN, H. J. & ANDREATCH, P. (1972) *J. Appl. Phys.*, 43, 2944.
- MITCHELL, A. C. & NELLIS, W. J. (1981) Shock Compression of aluminum, copper, and tantalum. *J. Appl. Phys.*, 52, 3363-3374.
- PIERMARINI, G. J., BLOCK, S., BARNETT, J. D. & FORMAN, R. A. (1975) Calibration of the pressure dependence of the R<sub>1</sub> ruby fluorescence line to 195 kbar. *J. Appl. Phys.*, 46, 2774 - 2780.
- ROZSNYAI, B. F., ALBRITTON, J. R., YOUNG, D. A. & SONNAD, V. N. (2001) Theory and experiment for ultrahigh pressure shock Hugoniots. *Phys. Lett A*, 291, 226.
- RUOFF, A. L., LINCOLN, R. C. & CHEN, Y. C. (1973) A new method of absolute high pressure determination. *J. Phys. D.*, 6, 1295.
- SYASSEN, K. (2004) unpublished notes.
- TALLON, J. L. & WOLFENDEN, A. (1979) Temperature dependence of the elastic constants of aluminum. *J. Phys. Chem. Solids*, 40, 831-837.

- VAN'T-KLOOSTER, P., TRAPPENIERS, N. J. & BISWAS, S. N. (1979) Effect of Pressure on the Elastic Constants of Noble Metals from  $-196$  to  $+25$  C and up to 2500 Bar: I. Copper. *Physica*, 97B, 65-75.
- WANG, Y. (2004) We thank Y. Wang for providing us with calculated thermal pressures for Al and W. *We thank Y. Wang for providing us with calculated thermal pressures for Al and W.*
- WANG, Y., AHUJA, R. & JOHANSSON, B. (2002) Reduction of shock-wave data with mean-field potential approach. *J. Appl. Phys.*, 92, 6616-6620.
- ZHA, C.-S., MAO, H. K. & HEMLEY, R. J. (2000) Elasticity of MgO and a primary scale to 55 GPa. *Proc. Nat. Acad. of Sciences*, 97, 13494-13499.